Liquid Crystals
Publication details, including instructions for authors and subscription information:
http://www.informaworld.com/smpp/title~content=t713926090

Synthesis and physical properties of a main-chain chiral smectic thiol-ene oligomer

Hong Yang[a]; Jacqueline M. Richardson[b]; David M. Walba[b]; Chenhui Zhu[c]; Renfan Shao[c]; Noel A. Clark[c]; Josu Ortega[d]; Jesus Etxebarria[e]; Patrick Keller[a]
[a] Institut Curie, Centre de Recherche, CNRS UMR 168, Université Pierre et Marie Curie, France [b] Department of Chemistry and Biochemistry, 215 UCB, University of Colorado, Boulder, CO, USA [c] Department of Physics, 390 UCB, University of Colorado, Boulder, CO, USA [d] Departamento de Física Aplicada II, Facultad de Ciencia y Tecnología, Universidad del País Vasco, Bilbao, Spain [e] Departamento de Física de la Materia Condensada, Facultad de Ciencia y Tecnología, Universidad del País Vasco, Apdo. 644, Bilbao, Spain

Online publication date: 04 March 2010

To cite this Article Yang, Hong , Richardson, Jacqueline M. , Walba, David M. , Zhu, Chenhui , Shao, Renfan , Clark, Noel A. , Ortega, Josu , Etxebarria, Jesus and Keller, Patrick(2010) 'Synthesis and physical properties of a main-chain chiral smectic thiol-ene oligomer', Liquid Crystals, 37: 3, 325 — 334
To link to this Article: DOI: 10.1080/02678290903511685
URL: http://dx.doi.org/10.1080/02678290903511685

Liquid Crystals,
Vol. 37, No. 3, March 2010, 325–334

Taylor & Francis
Taylor & Francis Group

Synthesis and physical properties of a main-chain chiral smectic thiol-ene oligomer

Hong Yang[a], Jacqueline M. Richardson[b], David M. Walba[b], Chenhui Zhu[c], Renfan Shao[c], Noel A. Clark[c], Josu Ortega[d], Jesus Etxebarria[e] and Patrick Keller[a]*

[a]*Institut Curie, Centre de Recherche, CNRS UMR 168, Université Pierre et Marie Curie, 26 rue d'Ulm 75248 Paris cedex 05, France;* [b]*Department of Chemistry and Biochemistry, 215 UCB, University of Colorado, Boulder, CO 80309-0215, USA;* [c]*Department of Physics, 390 UCB, University of Colorado, Boulder, CO 80309-0390, USA;* [d]*Departamento de Física Aplicada II, Facultad de Ciencia y Tecnología, Universidad del País Vasco, Apdo. 644, 48080, Bilbao, Spain;* [e]*Departamento de Física de la Materia Condensada, Facultad de Ciencia y Tecnología, Universidad del País Vasco, Apdo. 644, 48080, Bilbao, Spain*

(Received 13 November 2009; final version received 25 November 2009)

The synthesis and characterisation of a main-chain chiral smectic liquid crystalline thiol-ene polymer system is described. The chemical structure is designed based on the structure of **W317**, a mesogen with a large electroclinic effect in the Smectic A* (SmA*) phase. The novel thiol-ene monomer **K0902** has a large surface electroclinic effect with an unexpected small electroclinic effect in the SmA* phase. The corresponding thiol-ene oligomer poly-**K0902** is characterised by gel permeation chromatography (GPC), differential scanning calorimetry (DSC), polarised optical microscopy (POM), X-ray diffraction (XRD) and shows an expected I–SmA*–Glass phase sequence, but the electroclinic angle is relatively small.

Keywords: thiol-ene; oligomer; photopolymerisation; electroclinic effect

1. Introduction

Since the discovery by Garoff and Meyer [1] of the electroclinic effect in a chiral smectic A (SmA) mesophase in 1977, efforts have been pursued to apply this effect in building electromechanical actuators [2–4] and chirality sensors [5, 6]. However, most of the conventional Smectic A* (SmA*) materials exhibit small induced optical tilt angles (θ_{opt}) and small layer shrinkages, defining the X-ray tilts (θ_{xr}), under electric field [7]. On the other hand, de Vries SmA* materials with molecular directors randomly rotating along a tilt cone present small θ_{xr} but relatively large θ_{opt}, up to 30°, in response to fields of ~1 V μm^{-1} [8–13]. A non-de Vries SmA* material with a large electroclinic coefficient in the SmA* phase concomitant with a substantial layer shrinkage is highly desirable for electromechanical applications. However, very little data are available in the literature providing measurements of both optic and X-ray tilts as a function of the applied electric field to determine the 'de Vries' or 'non-de Vries' nature of SmA* materials [14–16].

The chiral calamitic liquid crystal (LC) mesogen, **W317** (Figure 1(a)), is a rare case of a non-de Vries SmA* material with a large electroclinic effect [17]. Based on the core structure of **W317**, a couple of specially designed polymers have been prepared showing consistently large electroclinic effects. Ratna and Naciri [4] successfully applied a photopolymerisation method to create a well-aligned side-chain LC elastomer, as shown in Figure 1(b), with an electroclinic effect up to 13° (the electroclinic coefficient, α, was calculated to be 0.34 V μm^{-1} at low applied fields (<20 V μm^{-1}) [4]. Walba *et al.* [18] prepared a main-chain LC polymer showing a large electroclinic effect (θ_{opt} ~23°, θ_{xr} ~21° in response to an electric field of 12 V μm^{-1} at 82°C, a temperature just above a SmA* to Smectic C* (SmC*) phase transition). However, the corresponding well-aligned main-chain LC elastomer network was difficult to achieve, because the chemical-polymerisation step and the photo-crosslinking step were separated into two different procedures, resulting in problems with aligning the very viscous polymer system in one uniform orientation. (Figure 1(c)) [19]. An ideal main-chain LC elastomer should be prepared by applying a one-step photopolymerisation on an already well-aligned LC monomer, a cross-linker and a photo-initiator mixture, just like Ratna and Naciri's side-chain network case [4].

Thiol-ene photopolymerisation is a well-known reaction for non-mesomorphic systems [20]. Lub *et al.* [21–23] and Wilderbeek *et al.* [24, 25] pioneered the synthesis and photopolymerisation of mesomorphic compounds containing vinyl and mercapto groups to give main-chain LC polymers. Recently, we used a thiol-ene photopolymerisation approach to prepare main-chain nematic liquid crystalline elastomers with ultra-large amplitude contractions [26]. We also synthesised a fluorinated main-chain chiral smectic thiol-ene polymer [27]. All of the above experiments proved that thiol-ene photopolymerisation could be a

*Corresponding author. Email: Patrick.keller@curie.fr

ISSN 0267-8292 print/ISSN 1366-5855 online

DOI: 10.1080/02678290903511685
http://www.informaworld.com

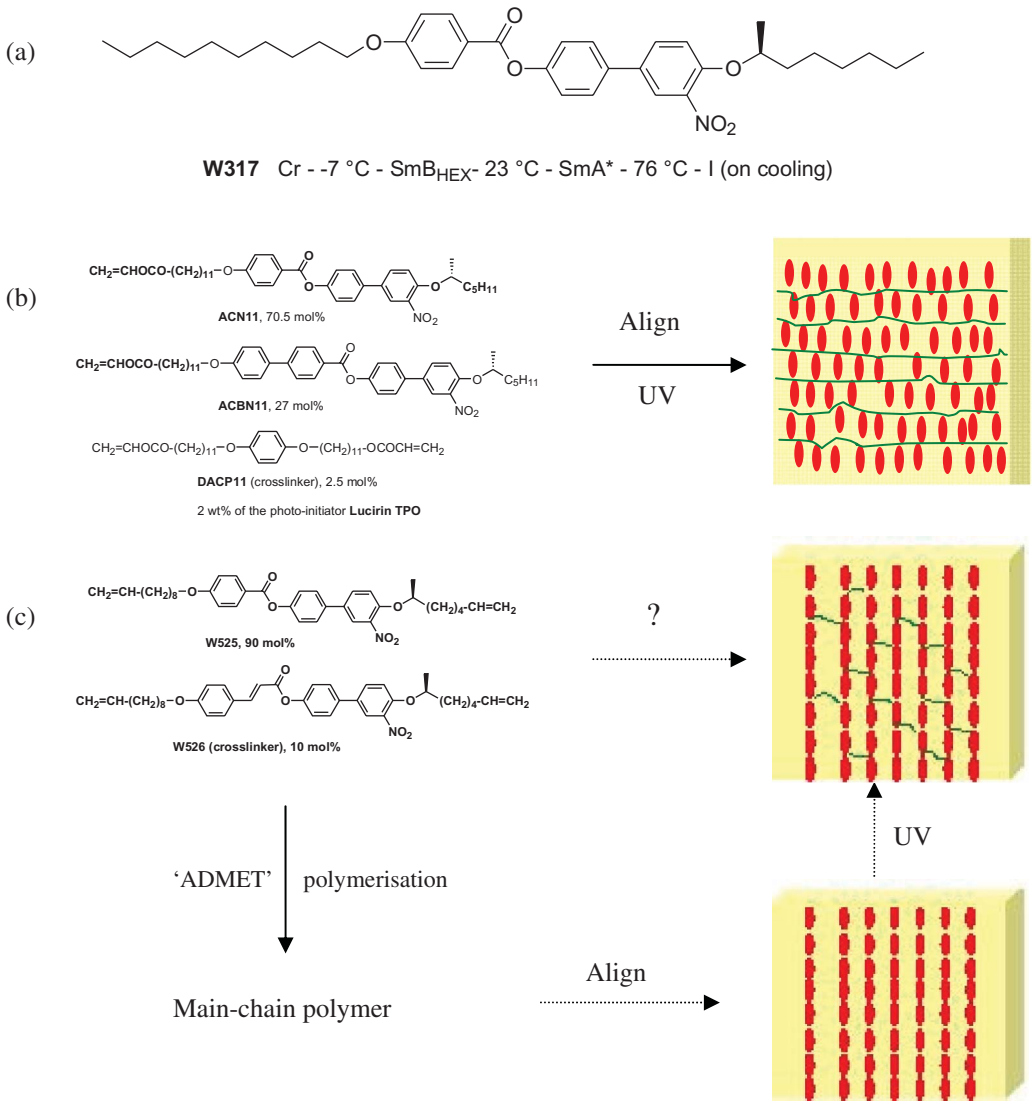

Figure 1. (a) The molecular structures and phase transitions of **W317**. (b) Ratna and Naciri's side-chain LC elastomer [4]. (c) Walba's main-chain LC polymer and proposed corresponding elastomer [19].

good approach to prepare well-aligned main-chain liquid crystalline electromechanical actuators in one step directly by ultraviolet (UV) illumination of the aligned mixtures of mesogenic monomers, cross-linkers and photoinitiators. Herein, we describe the design, synthesis and characterisation of a novel thiol-ene chiral smectic monomer (**K0902**) and the corresponding oligomer (poly-**K0902**), based on the core structure of the **W317** mesogen.

2. Synthesis

The synthesis route for **K0902** and poly-**K0902** is presented in Scheme 1. Controlled nitration of biphenyl-4,4′-diol (**1**) [24, 25] gave a mixture of the desired mono-nitro-biphenol **2**, along with di-nitrated product (80:20), after chromatography of the crude product. This mixture was carried forward without separation of the nitrophenols. Opening of the epoxide ring of unichiral epoxide **4** with the mixed cuprate derived from bromide **3** gave unichiral alcohol **5** in excellent yield [29, 30]. Regioselective Mitsunobu coupling [31] of alcohol **5** with nitrophenol **2** gave the desired nitrophenol ether **9** in 76% yield, calculated based upon the 80% purity of the starting mononitrodiphenol.

Etherification of ethyl-p-hydroxybenzoate (**6**) with 1,9-dibromononane (**7**), followed by acidic hydrolysis of the resulting ester, gave acid **8** [32]. Coupling of acid **8** with the phenolic nitroether **9** using the standard dicyclohexyl carbodiimide (DCC)/dimethylaminopyridine (DMAP) protocol [33] gave the mesogenic compound **10** in good yield.

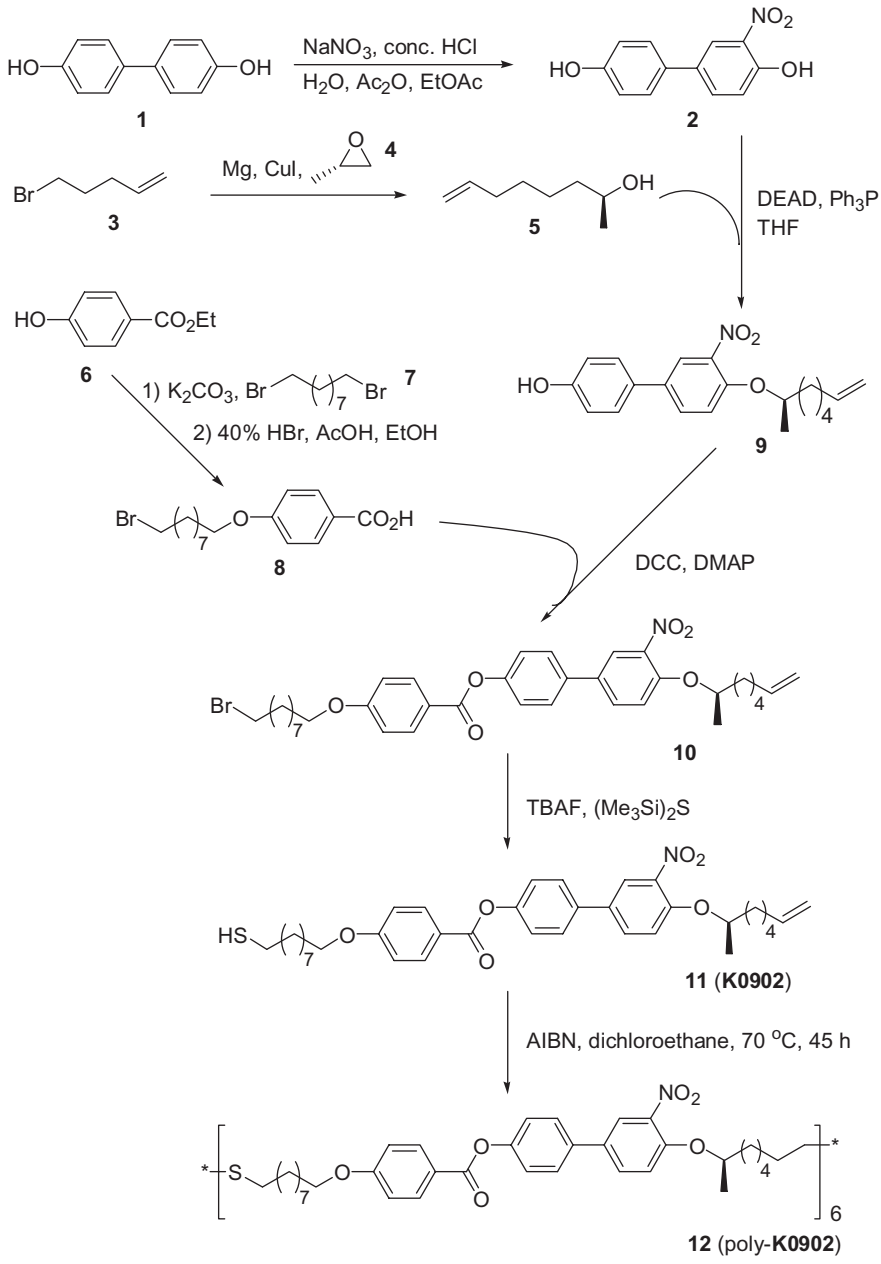

Scheme 1. Synthesis of monomer **K0902** and the corresponding oligomer poly-**K0902**.

The target monomer **11** (**K0902**) was finally synthesised by a very convenient trimethylsilylthioxy-dehalogenation reaction [34]. Azobis-isobutyronitrile (AIBN)-initiated polymerisation of monomer **11** in dichloroethane at 70°C for two days produced a main-chain oligomer **12** with a degree of polymerisation around 6. Details of the synthesis are given in Section 4.

3. Results and discussion

The thiol-ene monomer **K0902** exhibited the following phase transition behaviour (where SmB represents Smectic B), Cr – <–10°C –SmB_{HEX} – 5°C – SmA* – 50°C – I (on cooling, determined by polarised optical microscopy (POM)), which is similar to that of **W317** (Cr – –7°C –SmB_{HEX} – 23°C – SmA* – 76°C – I on cooling). **K0902** has a large surface electroclinic effect [35], which was not found in the case of **W317**. As shown in Figure 2, when **K0902** was filled by capillary suction in a 2.5 μm thick glass cell with only one surface rubbed, and cooled down from the isotropic to the smectic phase, the sample showed a uniform alignment with the layer normal rotated $\psi = 13^\circ$ from the rubbing direction, a consequence of the surface electroclinic effect $\theta_s \approx 13^\circ$ of

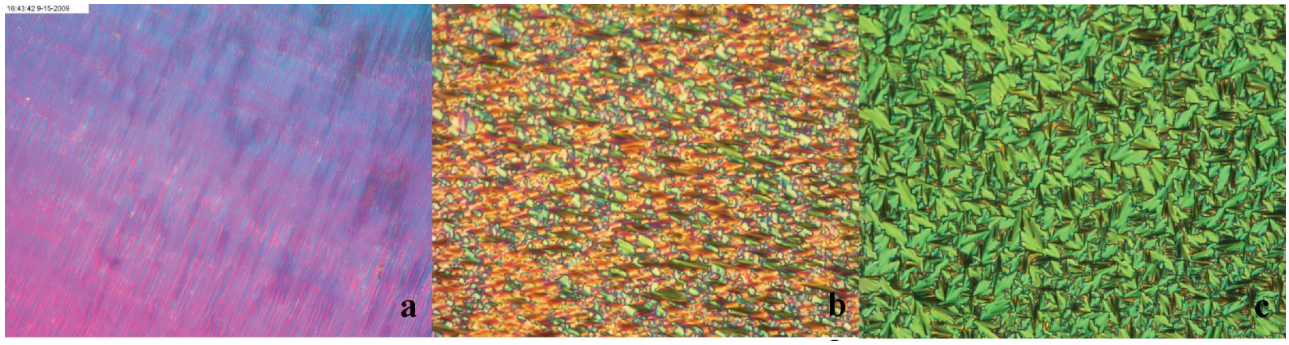

Figure 2. (a) The texture (40°C) of **K0902** filled in a 2.5 μm thick glass cell with one surface rubbed. (b) The texture (40°C) of **K0902** filled in a 4 μm thick glass cell with both surfaces parallel-rubbed. (c) The texture (40°C) of **K0902** filled in a 5 μm thick non-surface-treated glass cell.

the director (Figure 2(a)). The alignment in a 4 μm thick glass cell with both surfaces rubbed parallel was totally different (Figure 2(b)), because the different surface director tilts induced by the surface electroclinic effect prevented a uniform alignment of the director field [36]. Figure 2(c) showed a typical SmA fan-shaped texture of **K0902** filled in a 5 μm thick non-surface-treated glass cell. All of these textures were taken at 40°C, which was in the SmA* phase.

The polymerisation of **K0902** was carried out using toluene or dichloroethane as solvents. Different reaction temperatures and concentrations were tested. However, high molecular weight polymers were never obtained, as all of the experiments were consistently giving hexamers instead. We also tried to heat a neat mixture of **K0902** and AIBN, but the result was even worse, ending with a trimer. Similar polymerisation conditions gave previously relatively long nematic and smectic thiol-ene polymers (DP $>$ 20) [26, 27], while the specific failure reason in this case is unknown. A gel permeation chromatography (GPC) analysis versus polystyrene standards gave an amount of Mn $\sim$5.5 Kg mol^{-1} and a polydispersity index (PDI) of $\sim$1.73 (tetrahydrofuran (THF) as eluting solvent, 1.0 mL min^{-1}).

Poly-**K0902** was mesogenic, as indicated by POM and electro-optic behaviour in indium-tin oxide (ITO)/glass LC cells, where unaligned samples of polymer could be driven with an applied electric field. The sample was found to possess an I–SmA*–Glass phase sequence. A differential scanning calorimetry (DSC) experiment measured the exact phase transition temperatures as I – 98°C – SmA* – 9.2°C – Glass (Figure 3).

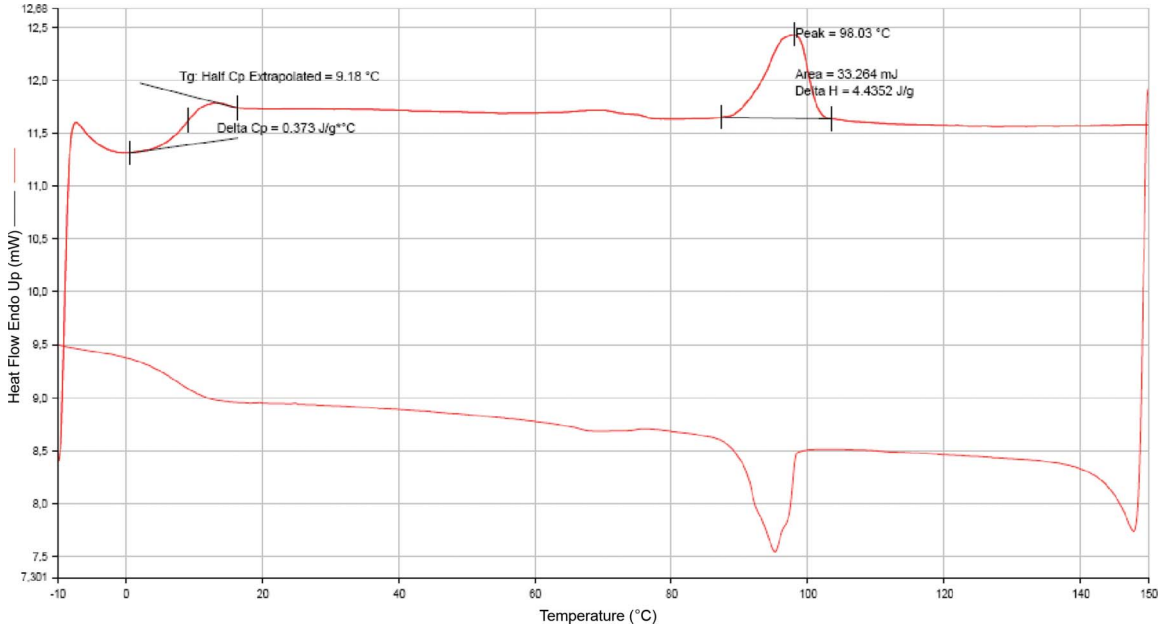

Figure 3. DSC thermogram of poly-**K0902**.

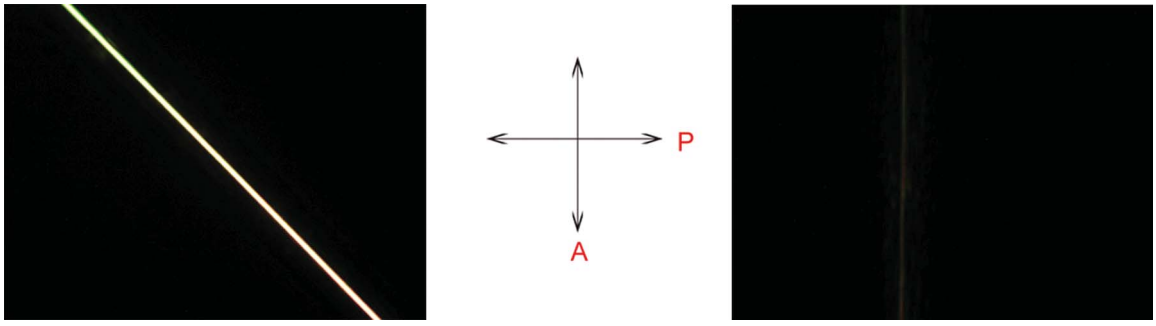

Figure 4. Photomicrographs of a glass fibre of polymer poly-**K0902** at room temperature observed between the crossed analyser (vertical) and polariser. The fibre diameter is ~40 μm.

Poly-**K0902** formed glassy smectic liquid crystalline fibres by pulling from the isotropic melt and then cooling down at room temperature. Figure 4 shows a well-aligned fibre with good extinction when the fibre axis is parallel or perpendicular to the polariser. Rotation of the fibre by 45° from extinction maximises the transmission.

The layer spacing as a function of temperature was measured for bulk (powder) samples of poly-**K0901**. As shown in Figure 5, this oligomer has a very small layer shrinkage with a smectic period of 3.32 nm below the I–SmA* phase transition and 3.22 nm at room temperature. After reaching a maximum in layer spacing at around 90°C, the interlayer distance decreased slightly until the SmA to isotropic transition temperature. This unusual behaviour could be related to the broad domain of transition seen by DSC (Figure 3) and is typical of a polydisperse polymer.

The electroclinic coefficient data of the monomer **K0902** was measured following a classical procedure [37]. The monomer was introduced by capillarity into a 5 μm thick glass cell at a temperature above its clearing point. Both glass surfaces had been treated with polyimide and rubbed unidirectionally. The material was then cooled down slowly (0.05°C min^{-1}) from the isotropic phase into the SmA* phase. Since the monomer has a large surface electroclinic effect, a bad alignment resulted in the mesophase (Figure 6). After subjecting the sample to a square-wave electric field (10 Hz, 50 V) for a few minutes a good alignment was obtained, with the molecular director along the rubbing direction (Figure 6). The sample was then placed between crossed polarisers with an angle of 22.5° between the director axis and the first polariser, and subjected to a sinusoidal voltage. The transmitted light was detected with a photodiode. The direct current (d.c.) component of the signal (I_0) was measured with a voltmeter and the alternating current (a.c.) component (I) with a lock-in amplifier. The tilt angle is simply $I/4I_0$.

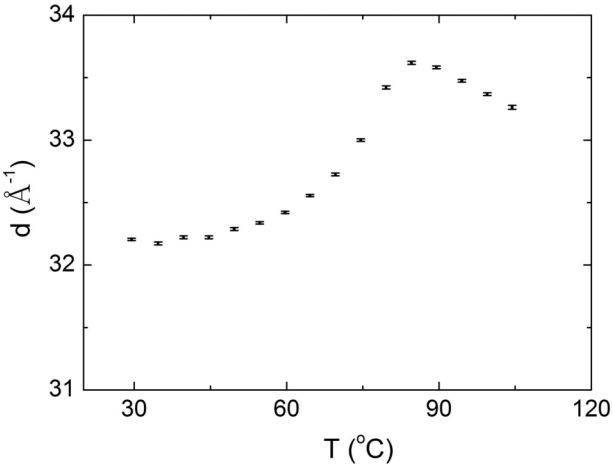

Figure 5. X-ray layer spacing (d) as a function of temperature for bulk samples of poly-**K0902**.

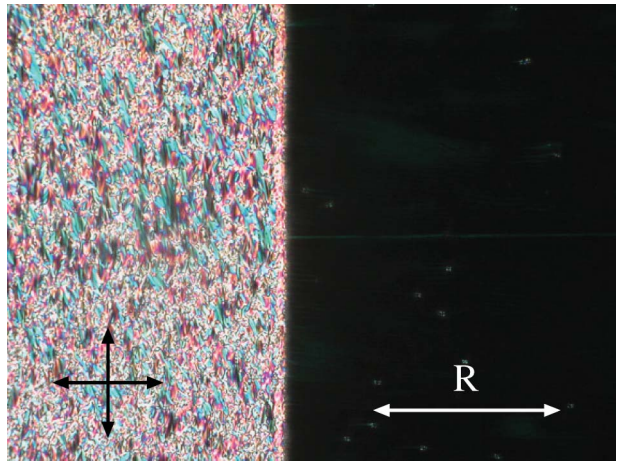

Figure 6. Textures of **K0902** at 27°C cooling from the isotropic phase at 0.05°C min^{-1} in a 5 μm thick cell, before (left-hand side) and after (right-hand side with ITO electrodes) applying a square-wave electric field (10 Hz, 50 V). (Both glass surfaces were treated with polyimide and rubbed unidirectionally. The black arrows indicate polariser directions and the white arrow is the rubbing direction R.)

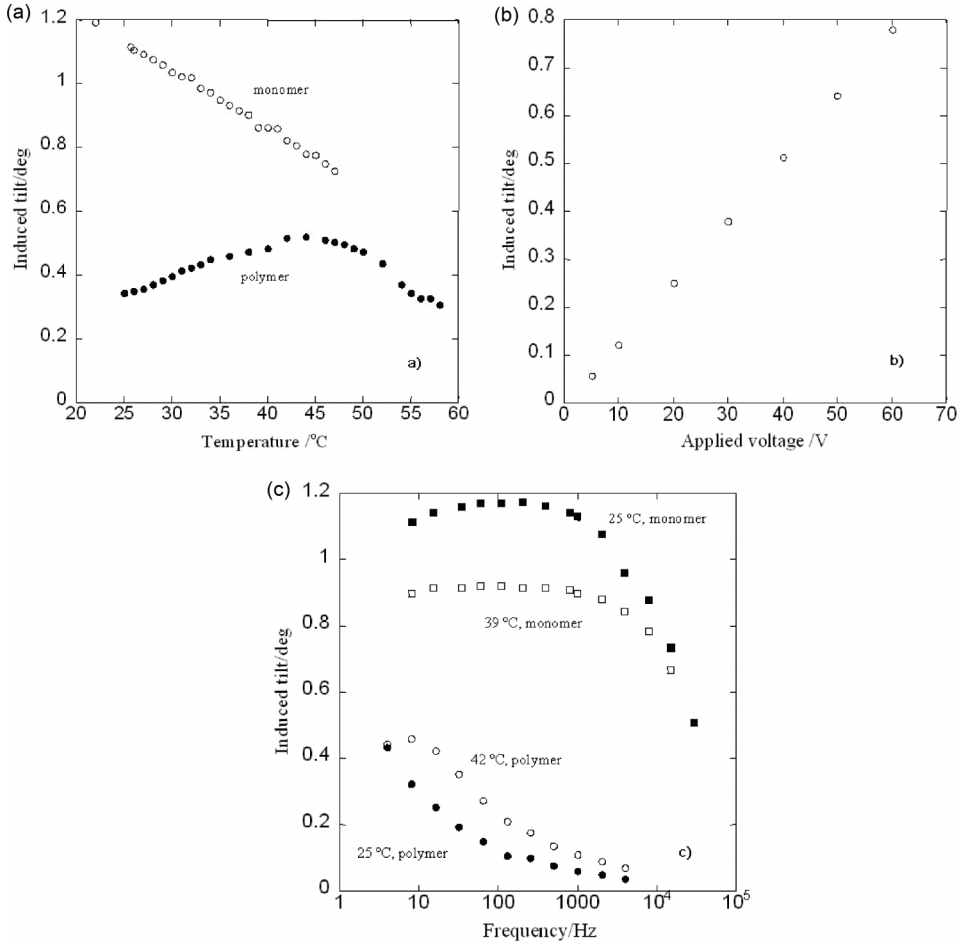

Figure 7. (a) Electroclinic effect in the SmA phase of the monomer **K0902** and the polymer poly-**K0902** (temperature dependence of the induced tilt for an applied voltage of 60 V, frequencies of 400 and 8 Hz, respectively). (b) Induced tilt in the SmA phase of the monomer at 44°C as a function of the applied field amplitude (400 Hz). (c) Relaxation behaviours of the monomer and the polymer at several temperatures within the SmA range.

The electroclinic coefficient data (Figure 7) of the polymer poly-**K0902** was measured following our previously reported procedure [27]. A mixture of the monomer **K0902** (99 mol%) and a commercially available photo-initiator, 2-benzyl-2-(dimethylamino)-4'-morpholinobutyrophenone (1 mol%) were prepared. The sample was filled in a glass cell, following the experimental procedure described above for the pure monomer, to achieve a good alignment. A polymer was then obtained by illuminating this well-aligned monomeric sample for 5 minutes with an UV lamp (30 $mW{\cdot}cm^{-2}$, $\lambda = 365$ nm, Electro-Cure 410). After illumination, the polymerisation was confirmed by checking that the clearing point had increased as expected (96°C). The sample alignment was good as proved by a rather uniform texture. The electroclinic effect data was obtained following the protocol described above.

Figure 7(a) shows the temperature dependence of the induced tilt angle of the monomer and the polymer for an applied voltage of 60 V, frequency of 400 Hz and 8 Hz, respectively. The induced tilt angle in **K0902** increased as the temperature decreased, reaching values around 1.2° near room temperature. At a given temperature, it increased as a linear function of the applied field amplitude (Figure 7(b)). The induced tilt angle values in poly-**K0902** are much smaller than those found for the monomer. Moreover, the apparently anomalous behaviour seen, a decrease of the induced tilt angle when the temperature is lowered from 45°C to 25°C, is mainly due to the fact that the electroclinic effect cannot even follow an 8 Hz frequency. This fact is clearer in Figure 7(c), which presents the frequency dependence of the induced tilt angle in the SmA phase of the monomer at 39°C (open squares) and 25°C (closed squares), as well as that for the polymer at

42°C (open circles) and 25°C (closed circles). The driving field was a sine wave of 60 V of amplitude in all cases. The monomer had a relaxation at frequencies 10–100 kHz. In contrast, the polymer relaxed at frequencies much smaller, particularly near room temperature, where the relaxation was well below 10 Hz.

The induced tilt angles in the **K0902** monomer and oligomer are very small compared with those of **W317**, **ACN11** and **W525** (Figure 1), which all have exactly the same core structure. This anomalous behaviour might derive from the thiol-ene tails, although the relationship between the presence of a thiol group and the drastic diminution of induced tilt angle is far beyond our current understanding.

4. Experimental details

4.1 General methods

For the mesogenic materials, the LC phases and phase transition temperatures were determined by polarised light microscopy using a Nicon-HCS400 microscope with an Instec-STC200 temperature-controlled stage or a Leitz Ortholux microscope equipped with a Mettler FP 82 hot stage. X-ray diffraction (XRD) experiments were conducted on Cu-K(alpha) radiation from a Rigaku UltraX-18 rotating anode generator, operated by the Liquid Crystal Materials Research Center, Boulder, Colorado.

New compounds in the synthetic route were routinely characterised by nuclear magnetic resonance (NMR) spectroscopy. ^{1}H NMR spectra were recorded at 500, 400 or 300 MHz, using $CDCl_3$ (internal reference 7.26 ppm) as the solvent. ^{13}C NMR spectra were obtained at 100 or 75M Hz using $CDCl_3$ (internal reference 77.23 ppm) as the solvent. All non-aqueous reactions were conducted in oven-dried glassware, under a dry argon atmosphere. CH_2Cl_2 was distilled from CaH_2 under nitrogen. THF was distilled from sodium-benzophenone ketyl under nitrogen. A Sigma 2K15 centrifuge was used for isolation of the polymers after precipitation. All flash chromatography was performed using Macherey-Nagel MN Kieselgel 60 (0.063–1.2 mm). Analytical thin-layer chromatography (TLC) was performed on E. Merck silica gel 60 F_{254} plates (0.25 mm). The compounds were visualised with UV or by staining with cerium ammonium molybdate, *p*-anisaldehyde, or $KMnO_4$ and heating.

*4.1.1 3-Nitro-biphenyl-4,4′-diol (**2**)*

Biphenyl-4,4′-diol (**1**) (10.0 g, 53.7 mmol) was dissolved in 500 mL of ethyl acetate. To the resulting solution was added $NaNO_3$ (5.0 g, 58.8 mmol) dissolved in H_2O (90 mL). Acetic anhydride (0.5 mL) was then added. To this mixture was added concentrated HCl (20.3 mL) dropwise. The two-phase reaction mixture was stirred at room temperature for 2 hours. Then, the layers were separated, and the aqueous layer was further extracted with ethyl acetate (3 × 200 mL). The combined organic layers were dried over anhydrous MgSO4, filtered, and then concentrated at reduced pressure to give a black oil. Purification of this crude product by flash chromatography (5:1 hexanes:ethyl acetate) gave a mixture of 3-Nitro-biphenyl-4,4′-diol and 3,3′-Dinitro-biphenyl-4,4′-diol (80% and 20%, respectively, based upon ^{1}H NMR analysis) as a dark orange solid (11.46 g, 88.9%). This material was used in the subsequent reaction without further purification. ^{1}H NMR (500 MHz, CDCl3): δ 10.53 (d, 1H, $J = 6.00$ Hz), 8.23 (d, 1H, $J = 2.29$ Hz), 7.76 (dd, 1H, $J = 2.30$, 8.70 Hz), 7.42 (AA'BB', 2H), 7.35 (d, 1H, $J = 8.69$ Hz), 6.90 (AA'BB', 2H). ^{13}C NMR (100 MHz, CDCl3): δ 164.9, 152.9, 143.0, 134.1, 133.1, 131.8, 130.2, 128.7, 128.6, 120.7.

*4.1.2 (S)-Oct-7-en-2-ol (**5**)*

A crystal of I_2 was added to pre-dried Mg turnings (1.1 g, 45.26 mmol) under argon. A solution of 5-bromo-1-pentene (**3**) (6.54 g, 43.9 mmol) in 20 mL dry THF was slowly added to the Mg under argon over a period of 2 hours, which caused gentle refluxing of the solution. After completion of the addition, the mixture was stirred for 1 hour at 25°C, and 0.5 hour at 0°C. Solid CuI (fresh) (0.795 g, 2.37 mmol) was then added to the solution, which was stirred for 0.5 hour before the slow addition of a solution of (S)-(-)-Propylene oxide (**4**) (1.968 g, 33.88 mmol) in 12 mL dry THF, keeping the temperature at 0°C. The reaction mixture was stirred for an additional 3 hours at 0°C, then poured into saturated NH_4Cl solution, stirred for 1 hour, extracted with Et_2O, and dried with $MgSO_4$. The filtration and removal of solvents by rotary evaporation gave an oil, which was directly subjected to purification by flash chromatography (4:1 hexanes:ethylacetate) to provide (S)-oct-7-en-2-ol (**5**) (4.08 g, 94%) as a colourless oil. ^{1}H NMR (500 MHz, $CDCl_3$): δ 5.75–5.81 (m, 1H), 4.91–5.00 (m, 2H), 3.75–3.78(m, 1H), 2.02–2.06 (m, 2H), 1.30–1.47 (m, 6H), 1.17 (d, 3H, $J = 6.00$ Hz). ^{13}C NMR (100 MHz, $CDCl_3$): δ 138.7, 114.2, 67.8, 40.0, 33.6, 28.8, 25.1, 23.3.

*4.1.3 (R)-4′-(1-Methyl-hept-6-enyloxy)-3′-nitro-biphenyl-4-ol (**9**)*

Diethylazodicarboxylate (DEAD) (6.858 mL, 42.25 mmol) was added via a syringe with stirring and under argon to a solution of a mixture of 3-nitro-biphenyl-4,4′-diol (**2**) and dinitro-diol prepared as

described above (7.51 g total, containing 6.0 g, 25.0 mmol **2**, the remaining being the dinitrod:phenol), (S)-oct-7-en-2-ol (**5**) (5.00 g, 39.0 mmol) and triphenyl phosphine (TPP) (11.2 g, 42.25 mmol) in 300 mL dry THF. The reaction mixture was stirred for 12 hours at 25°C, and was then concentrated by rotary evaporation to give an orange oil, which was directly subjected to purification by flash chromatography (20:1 hexanes:ethylacetate) to provide (R)-4′-(1-methyl-hept-6-enyloxy)-3′-nitro-biphenyl-4-ol (**9**) (6.78 g, 76% based on nitrodiol **2**) as an orange oil. ^{1}H NMR (500 MHz, $CDCl_3$): δ 7.92 (d, 1H, $J = 2.39$ Hz), 7.62 (dd, 1H, $J =$ 2.39, 8.71 Hz), 7.39 (AA'BB', 2H), 7.07 (d, 1H, $J =$ 8.89 Hz), 6.89 (AA'BB', 2H), 5.77 (m, 1H), 5.18 (s, 1H), 4.96 (m, 2H), 4.50 (m, 1H), 2.04 (m, 2H), 1.78 (m, 1H), 1.63 (m, 1H), 1.41 (m, 4H), 1.35 (d, 3H, $J = 6.13$ Hz). ^{13}C NMR (100 MHz, $CDCl_3$): δ 155.7, 150.6, 141.2, 139.0, 133.4, 131.9, 131.5, 128.2, 123.6, 116.4, 116.2, 114.8, 76.7, 36.3, 33.8, 29.0, 25.0, 19.8.

*4.1.4 4-(9-Bromo-nonyloxy)-benzoic acid (**8**)*

A 100 mL round bottom flask was charged with 4-hydroxy-benzoic acid ethyl ester (**6**) (6.00 g, 35.7 mmol), 1,9-dibromononane (**7**) (10.54 g, 35.7 mmol) and K_2CO_3 (7.40 g, 53.5 mmol) in 25 mL 2-butanone. The reaction mixture was stirred for 18 hours at 80°C and then filtered. The resulting solution was concentrated to an oil, which was directly subjected to purification by flash chromatography (25:1 hexanes:ethylacetate) to provide 4-(9-Bromo-nonyloxy)-benzoic acid ethyl ester (4.85 g, 13.1 mmol) as a white solid. A 250 mL round bottom flask was charged with 4-(9-Bromo-nonyloxy)-benzoic acid ethyl ester (4.85 g, 13.1 mmol), 24 mL 40% hydrobromic acid aqueous solution, 60 mL acetic acid and 12 mL ethanol. The reaction mixture was refluxed for 18 hours and then cooled in an ice bath until a large mass of solid appeared. The solid was filtered, washed by water and dried under high vacuum to give pure 4-(9-Bromo-nonyloxy)-benzoic acid (3.37 g, 27.6% over two steps) as a white solid; mp 136°C. ^{1}H NMR (300 MHz, $CDCl_3$): δ 8.04 (AA'BB', 2H), 6.93 (AA'BB', 2H), 4.02 (t, 2H, $J = 6.49$ Hz), 3.41 (t, 2H, $J = 6.84$ Hz), 1.83 (m, 4H), 1.39, (m, 10H). ^{13}C NMR (75 MHz, $CDCl_3$): δ 171.5, 163.6, 132.3, 121.3, 114.2, 68.2, 34.0, 32.8, 29.3, 29.2, 29.1, 28.7, 28.1, 25.9.

*4.1.5 (R)-4-(9-Bromo-nonyloxy)-benzoic acid 4′-(1-methyl-hept-6-enyloxy)-3′-nitro-biphenyl-4-yl ester (**10**)*

A solution of DCC (595 mg, 2.89 mmol) in 10 mL dry CH_2Cl_2 was added via a syringe with stirring and under argon to a solution of (R)-4′-(1-methyl-hept-6-enyloxy)-3′-nitro-biphenyl-4-ol (**9**) (1.13 g, 3.28 mmol), 4-(9-Bromo-nonyloxy)-benzoic acid (**8**) (896 mg, 2.62 mmol) and DMAP (64 mg, 0.52 mmol) in 20 mL dry CH_2Cl_2. The reaction mixture was stirred for 12 hours at 25°C, and then concentrated by rotary evaporation to give the crude product as an oil, which was directly subjected to purification by flash chromatography (20:1 hexanes:ethylacetate) to provide 4-(9-Bromo-nonyloxy)-benzoic acid 4′-(1-methyl-hept-6-enyloxy)-3′-nitro-biphenyl-4-yl ester (**10**) (1.27 g, 72.9%) as a yellow wax-like solid. ^{1}H NMR (300 MHz, $CDCl_3$): δ 8.16 (AA'BB', 2H), 8.00 (d, 1H, $J =$ 2.34 Hz), 7.69 (dd, 1H, $J = 2.35$, 8.72 Hz), 7.58 (AA'BB', 2H), 7.27 (AA'BB', 2H), 7.13 (d, 1H, $J =$ 8.94 Hz), 6.98 (AA'BB', 2H), 5.79 (m, 1H), 4.96 (m, 2H), 4.54 (m, 1H), 4.06 (t, 2H, $J = 6.50$ Hz), 3.42 (t, 2H, $J = 6.83$ Hz), 2.06 (m, 2H), 1.84 (m, 5H), 1.66 (m, 1H), 1.40 (m, 14H), 1.38 (d, 3H, $J = 5.70$ Hz). ^{13}C NMR (75 MHz, $CDCl_3$): δ 164.9, 163.6, 150.8, 141.1, 138.7, 136.1, 132.6, 132.3, 132.0, 127.8, 123.8, 122.4, 121.3, 116.1, 114.5, 114.3, 68.3, 36.1, 34.1, 33.7, 32.8, 29.3, 29.2, 29.1, 28.8, 28.7, 28.1, 26.0, 24.7, 19.6. Phase sequence and transition temperatures: Cr – 33.2°C – SmA* – 42.5°C – I (on cooling, determined by POM).

*4.1.6 (R)-4-(9-Mercapto-nonyloxy)-benzoic acid 4′-(1-methyl-hept-6-enyloxy)-3′-nitro-biphenyl-4-yl ester (**11**)*

A solution of 4-(9-Bromo-nonyloxy)-benzoic acid 4′-(1-methyl-hept-6-enyloxy)-3′-nitro-biphenyl-4-yl ester (**10**) (1.19 g, 1.79 mmol) in 50 mL dry THF was cooled to −10°C under argon. Hexamethyldisilathiane (0.45 mL, 2.15 mmol) and tetra-*n*-butylammonium fluoride (TBAF) (1M solution in THF, 1.97 mL, 1.97 mmol) were added via a syringe. The reaction mixture was stirred for 10 minutes at −10°C, and then quickly poured into a saturated ammonium chloride solution. The resulting solution was extracted by ethyl acetate (200 mL, three times). The combined organic solutions were washed with brine, dried over sodium sulphate and then concentrated by rotary evaporation to give crude product as an oil, which was directly subjected to purification by flash chromatography (20:1 hexanes:ethylacetate) to provide 4-(9-Mercapto-nonyloxy)-benzoic acid 4′-(1-methyl-hept-6-enyloxy)-3′-nitro-biphenyl-4-yl ester (**11**) (0.91 g, 82.3%) as a yellow wax-like solid. ^{1}H NMR (300 MHz, CDCl3): δ 8.16 (AA'BB', 2H), 8.00 (d, 1H, $J = 2.33$ Hz), 7.70 (dd, 1H, $J = 2.36$, 8.72 Hz), 7.58 (AA'BB', 2H), 7.27 (AA'BB', 2H), 7.13 (d, 1H, $J = 8.94$ Hz), 6.98 (AA'BB', 2H), 5.79 (m, 1H), 4.98 (m, 2H), 4.55 (m, 1H), 4.05 (t, 2H, $J = 6.50$ Hz), 2.53 (q, 2H, $J = 7.19$, 7.42 Hz), 2.07 (m, 2H),

1.83 (m, 3H), 1.62 (m, 3H), 1.46 (m, 14H), 1.35 (d, 3H, J = 5.72 Hz). ^{13}C NMR (75 MHz, $CDCl_3$): δ 164.9, 163.6, 150.8, 141.1, 138.7, 136.1, 132.6, 132.3, 132.0, 127.8, 123.8, 122.4, 121.3, 116.1, 114.5, 114.3, 68.3, 36.1, 34.0, 33.6, 29.4, 29.3, 29.1, 29.0, 28.7, 28.3, 26.0, 24.8, 24.7, 19.6. Phase sequence and transition temperatures: Cr – <–10°C – SmB_{HEX} – 5°C – SmA* – 50°C – I (on cooling, determined by POM).

*4.1.7 Oligomer **12** ($n \sim 6$)*

To a solution of 4-(9-Mercapto-nonyloxy)-benzoic acid 4′-(1-methyl-hept-6-enyloxy)-3′-nitro-biphenyl-4-yl ester (**11**) (189 mg, 0.31 mmol) in 0.7 mL dichloroethane was added AIBN (2.51 mg, 0.015 mmol) under argon. The reaction mixture was purged by argon and then sealed in a pressure tube, which was heated at 70°C for 45 hours. The polymer product was then precipitated from the solution by the addition of a large amount of methanol. The product was then separated from the solution by centrifugation, providing oligomer **12** ($n \sim 6$ by end group analysis using ^{1}H NMR) as a white powder (120 mg, 72.3%). ^{1}H NMR (300 MHz, $CDCl_3$): δ 8.15 (m, 12H), 7.99 (d, 6H, J = 1.73 Hz), 7.69 (dd, 6H, J = 1.95, 8.67 Hz), 7.57 (AA'BB', 12H), 7.27 (AA'BB', 12H), 7.12 (d, 6H, J = 8.92 Hz), 6.97 (AA'BB', 12H), 5.80 (m, 1H), 4.98 (m, 2H), 4.54 (m, 6H), 4.04 (t, 12H, J = 6.39 Hz), 2.68 (m, 1H), 2.50 (t, 22H, J = 7.27 Hz), 2.07 (m, 2H), 1.46 (m, 144H). Phase transitions: SmA* – 97°C – I (on cooling, determined by POM).

5. Conclusion

Thiol-ene photopolymerisation is a unique method to prepare main-chain liquid crystalline polymers via a photopolymerisation procedure. This technique paves the way for the easy preparation of well-aligned main-chain liquid crystalline polymers and elastomers, which are usually very difficult to obtain. It is obvious that the potentialities of thiol-ene liquid crystalline materials have not been fully explored yet.

The story of **K0902** is one of our initial researches on thiol-ene liquid crystalline materials. We hope that the synthetic protocol, the thiol-ene mixtures alignment and the photopolymerisation procedure described here set a good start to this very promising LC research field. Moreover, the mystery of the small electroclinic effect obtained by associating a 'good' mesogenic core and the thiol-ene tails remains to be solved.

Acknowledgements

We thank the Agence Nationale de la Recherche (award No. ANR-07-MAPR-0020-02) and the Liquid Crystal Materials Research Center (NSF MRSEC Award No. DMR-0213918) for partial financial support of this work.

References

[1] Garoff, S.; Meyer, R.B. *Phys. Rev. Lett.* **1977**, *38*, 848–851.
[2] Lehmann, W.; Skupin, H.; Tolksdorf, C.; Gebhard, E.; Zentel, R.; Kruger, P.; Losche, M.; Kremer, F. *Nature* **2001**, *410*, 447–450.
[3] Kohler, R.; Stannarius, R.; Tolksdorf, C.; Zentel, R. *Appl. Phys. A: Mater. Sci. Process* **2005**, *90*, 381–388.
[4] Spillmann, C.M.; Ratna, B.R.; Naciri. J. *Appl. Phys. Lett.* **2007**, *90*, 021911.
[5] Walba, D.M.; Eshdat, L.; Korblova, E.; Shao, R.; Clark, N.A. *Angew. Chem., Int. Ed.* **2007**, *46*, 1473–1475.
[6] Kapernaum, N.; Walba, D.M.; Korblova, E.; Zhu, C.; Jones, C.; Shen, Y.; Clark, N.A.; Giesselmann, F. *Chemphyschem* **2009**, *10*, 890–892.
[7] Walba, D.M.; Korblova, E.; Eshdat, L.; Biewer, M.C.; Yang, H.; Jones, C.; Nakata, M.; Talarico, M.; Shao, R.; Clark, N.A. *J. Soc. Inf. Display* **2007**, *15*, 585–588.
[8] de Vries, A.; Ekachai, A.; Spielberg, N. *Mol. Cryst. Liq. Cryst. Lett.* **1979**, *49*, 143–152.
[9] de Vries, A. *Mol. Cryst. Liq. Cryst. Lett.* **1979**, *49*, 179–185; de Vries, A. *Mol. Cryst. Liq. Cryst.* **1977,** *41*, 27–31.
[10] Clark, N.A.; Bellini, T.; Shao, R.; Coleman, D.; Bardon, S.; Link, D.R.; Maclennan, J.E.; Chen, X.-H.; Wand, M.D.; Walba, D.M.; Rudquist, P.; Lagerwall, S.T. *Appl. Phys. Lett.* **2002**, *80*, 4097–4099.
[11] Xue, J.; Walba, D.M. Ferroelectric liquid crystal devices using materials with a de Vries smectic A phase. *US Patent No. 6,870,163*, Mar. 22, 2005.
[12] Lagerwall, J.P.F.; Coleman, D.; Korblova, E.; Jones, C.; Shao, R.; Oton, J.M.; Walba, D.M.; Clark, N.A.; Giesselmann, F. *Liq. Cryst.* **2006**, *33*, 17–23.
[13] Wand, M.D.; More, K.M.; Thurmes, W.N. *Use of Germanium FLCs in Search of the Perfect FLC Display*, Abstracts, 10th International Ferroelectric Liquid Crystal Conferences, Stare Jablonki, Poland, Institute of Applied Physics and Institute of Chemistry, Military University of Technology: Warsaw, Poland, 2005; p. O26.
[14] Rappaport, A.G.; Williams, P.A.; Thomas, B.N.; Clark, N.A.; Ros, M.B.; Walba, D.M. *Appl. Phys. Lett.* **1995**, *67*, 362–364.
[15] Shashidhar, R.; Naciri, J.; Ratna, B.R. *Adv. Chem. Phys.* **2000**, *113*, 51–76.
[16] Spector, M.S.; Heiney, P.A.; Naciri, J.; Weslowski, B.T.; Holt, D.B.; Shashidhar, R. *Phys. Rev. E: Stat., Nonlinear, Soft Matter Phys.* **2000**, *61*, 1579–1584.
[17] Williams, P.A.; Komitov, L.; Rappaport, A.G.; Thomas, B.N.; Clark, N.A.; Walba, D.M.; Day, G.W. *Liq. Cryst.* **1993**, *14*, 1095–1105.
[18] Walba, D.M.; Yang, H.; Shoemaker, R.K.; Keller, P.; Coleman, D.A.; Jones, C.D.; Nakata, M.; Clark, N.A. *Chem. Mater.* **2006**, *18*, 4576–4584.
[19] Yang, H. Main Chain Chiral Smectic Liquid Crystalline Polymers for Electro-Mechanical and

NLO Application. *Ph.D. Dissertation*. Univ. Colorado, Boulder, 2007.
[20] Hoyle, C.E.; Lee, T.Y.; Roper, T. *J. Polym. Sci., Part A: Polym. Chem.* **2004**, *42*, 5301–5338.
[21] Lub, J.; Broer, D.J.; Van Den Broek, N. *Liebigs Ann.* **1997**, 2281–2288.
[22] Lub, J.; Broer, D.J.; Martinez Antonio, M.E.; Mol, G.N. *Liq. Cryst.* **1998**, *24*, 375–379.
[23] Lub, J.; Broer, D.J.; Allan, J.F. *Mol. Cryst. Liq. Cryst.* **1999**, *332*, 259–266.
[24] Wilderbeek, H.T.A.; Goossens, J.G.P.; Bastiaansen, C.W.M.; Broer, D.J. *Macromolecules* **2002**, *35*, 8962–8968.
[25] Wilderbeek, H.T.A.; Van Der Meer, M.G.M.; Jansen, M.A.G.; Nelissen, L.; Fischer, H.R.; Van Es, J.J.G.S.; Bastiaansen, C.W.M.; Lub, J.; Broer, D.J. *Liq. Cryst.* **2003**, *30*, 93–108.
[26] Yang, H.; Buguin, A.; Taulemesse, J.M.; Kaneko, K.; Mery, S.; Bergeret, A.; Keller, P. *J. Am. Chem. Soc.* **2009**, *131*, 15000–15004.
[27] Yang, H.; Wang, L.; Shao, R.; Clark, N.A.; Ortega, J.; Etxebarria, J.; Albouy, P.A.; Walba, D.M.; Keller, P. *J. Mater. Chem.* **2009**, *19*, 7208–7215.
[28] Keller, P. *Bull. Soc. Chim. Fr.* **1994**, *131*, 27–29.
[29] Johnston, B.D.; Slessor, K.N. *Can. J. Chem.* **1979**, *57*, 233–235.
[30] Kandil, A.A.; Slessor, K.N. *Can. J. Chem.* **1983**, *61*, 1166–1168.
[31] Mitsunobu, O. *Synthesis* **1981**, 1–28.
[32] Ishikawa, Y.; Kunitake, T. *J. Am. Chem. Soc.* **1991**, *113*, 621–630.
[33] Neises, B.; Steglich, W. *Angew. Chem.* **1978**, *90*, 556–557.
[34] Hu, J.; Fox, M.A. *J. Org. Chem.* **1999**, *64*, 4959–4961.
[35] Xue, J.; Clark, N.A. *Phys. Rev. Lett.* **1990**, *64*, 307–310.
[36] Shao, R.; Maclennan, J.E.; Clark, N.A.; Dyer, D.J.; Walba, D.M. *Liq. Cryst.* **2001**, *28*, 117–123.
[37] Qiu, R.; Ho, J.T.; Hark, S.K. *Phys. Rev. A: At., Mol., Opt. Phys.* **1988**, *38*, 1653–1655.